International Journal of Sustainable Construction Engineering & Technology
Vol 1, No 2, December 2010

Ultra-High Performance 'Ductile' Concrete Technology Toward Sustainable Construction

Yen Lei Voo*

Director & CEO, Dura Technology Sdn. Bhd., Perak, Malaysia

*Corresponding Email: dura@dura.com.my

ABSTRACT

This paper briefly presents an overview of the material characteristics of a Malaysia blend of ultra-high performance 'ductile' concrete (UHPdC) know as DURA®. Examples of the environmental impact calculations of UHPdC structures compared to that of conventional reinforced concrete design are presented. The comparison studies show that many structures constructed from UHPdC are generally more environmentally sustainable than built of the conventional reinforced concrete with respect to the reduction of CO_2 emissions and embodied energy. The enhanced durability of UHPdC also provides for significant improvements in the design life, which further supporting the concept of sustainable construction.

Keyword: *Ultra-high performance ductile concrete, ductility, durability, embodied energy, CO_2, chloride.*

**Corresponding Author*

1.0 INTRODUCTION

'Environmental Friendly', 'Eco-', 'Green', 'Sustainable', 'Recycle' – are important contemporary keywords. They are associated with almost everything that we see, hear and feel. It is the view of many notable scientists, engineers, politicians and also of the community at large that mother earth is at the brink of needing another revolution; a revolution to sustain! With continuous efforts in extracting natural resources and discharging of wastes, we see and are starting to experience the result of human deeds, albeit good intentioned, through climate change or global warming to be exact. With the current stage of the planets environmental development; temperature rising, water level rising, natural disasters happening in unexpected parts of the world, food and clean water scarcity, diseases, limited natural resources, animal extinction, and growing human population, it is little wonder that the scientific community have issued warnings that the planet is in need of help.

On the positive side, the issues that societies are faced with provide innovation drivers for a range of new '*green*' technologies. The principle of sustainable construction stands on a basis of material optimization together with structural design optimization, which results in the lowest life-cycle cost. Figure 2 shows some of the immediate and long-term benefits that UHPdC technology is able to provide in the build and construction field. In short, this technology focuses on the reduction of none-renewable resources consumption couple with the used of recycle material; enhanced functionality of a structure through enhancement of service life and durability.

Over the last two decades, amazing progress has been made in concrete technology. One of the major breakthroughs of the 1990s was the development of ultra-high performance ductile concrete (UHPdC), also known as the reactive powder concrete (RPC), by Richard and Cheyrezy [1, 2]. Compressive strengths and flexural strength of over 180 MPa and 40 MPa, respectively, have been reported. Since then, extensive research studies have been undertaken by academics and engineers alike with the view to industrialize this technology as an alternative for sustainable construction.

This paper firstly presents an overview on the material characteristics of a Malaysian blend of ultra-high performance 'ductile' concrete (UHPdC), known as DURA®. Secondly, examples on the environmental impact calculation (EIC) of UHPdC structures are compared against comparable structures build using conventional methods. Lastly, the durability aspects are discussed and design calculations presented.

2.0 MATERIAL CHARACTERISTICS OF UHPdC

Ultra-high performance 'ductile' concrete (UHPdC) is suitable for use in the production of precast elements for civil and structural engineering and architectural applications. It is a highly homogenous cementitious based composite without coarse aggregates that can achieve compressive strengths of greater than 150 MPa. Its blend of very high strength micro-steel fibers and cementitious binders with extremely low water content give UHPdC extraordinary characteristics of mechanical strengths comparable to steel, high ductility and with a durability comparable to natural rocks.

Error! Reference source not found. summarizes the material characteristics of UHPdC and is compared against conventional, or normal, strength concrete (NSC) and high performance concrete (HPC). The comparison shows that UHPdC have superior mechanical properties over NSC and HPC in all aspects.

The components of UHPdC are ordinary Portland cement, silica fume, fine aggregate, water, steel fibers and a high-range water reducing agent. In order to achieve the required performance of UHPdC, powder materials and fine aggregates are blended or proportioned to an adequate particle size distribution in order to maximize the density or compactness. Table 1 – **Material characteristics of UHPdC compared to normal strength concrete (NSC) and high performance concrete (HPC)**

Characteristics	Unit	Codes / Standards	NSC	HPC	DURA® - UHPdC
Specific Density, □	kg/ m3	BS1881-Part 114, 1983 [3]	2300	2400	2350 – 2450
Cylinder Compressive Strength, *fcy*	MPa	AS1012.9, 1999 [4]	20 – 50	50 – 100	120 – 160
Cube Compressive Strength, *fcc*	MPa	BS6319-Part 2, 1983 [5]	20 – 50	50 – 100	130 – 170
Creep Coefficient at 28 days, □□□		AS1012.16, 1996 [6]	2 – 5	1 – 2	0.2 – 0.5
Post Cured Shrinkage	□□	AS1012.16, 1996 [6]	1000 – 2000	500 – 1000	< 100
Modulus of Elasticity, *Eo*	GPa	BS1881-Part 121, 1983 [7]	20 – 35	35 – 40	40 – 50
Poisson's Ratio, □			0.2	0.2	0.18 – 0.2
Split Cyl. Cracking Strength, *ft*	MPa	BS EN 12390-6, 2000 [8] ASTM C496, 2004 [9]	2 – 4	4 – 6	5 – 10
Split Cyl. Ultimate Strength, *fsp*	MPa		2 – 4	4 – 6	10 – 18
Flexural 1st Cracking Strength, *fcr,4P*	MPa	ASTM C1018, 1997 [10] (Four-Point Test on Un-notched Specimen)	2.5 – 4	4 – 8	8 – 9.3
Modulus of Rupture, *fcf,4P*	MPa		2.5 – 4	4 – 8	18 – 35
Bending Fracture Energy, *Gf,d=0.46mm*	N/mm		< 0.1	< 0.2	1 – 2.5
Bending Fracture Energy, *Gf,d=3.0mm*	N/mm		< 0.1	< 0.2	10 – 20
Bending Fracture Energy, *Gf,d=10mm*	N/mm		< 0.1	< 0.2	15 – 30
Toughness Indexes *I5*			1	1	4 – 6
Toughness Indexes *I10*			1	1	10 – 15
Toughness Indexes *I20*			1	1	20 – 35
Modulus of Rupture, *fcf,3P*	MPa	JCI-S-002, 2003 [11] (Three-Point Test on Notched Specimen)	2.5 – 4	4 – 8	18 – 35
Bending Fracture Energy, *Gf,d=0.46mm*	N/mm		<0.1	<0.2	1 – 2.5
Bending Fracture Energy, *Gf,d=3.0mm*	N/mm		<0.1	<0.2	10 – 20
Bending Fracture Energy, *Gf,d=10mm*	N/mm		<0.1	<0.2	15 – 30
Rapid Chloride Permeability	coul omb	ASTM C1202, 2005	2000 – 4000	500 – 1000	< 200

		[12]			
Chloride Diffusion Coefficient, *Dc*	mm 2/s	ASTM C1556, 2004 [13]	4 – 8 x 10-6	1 – 4 x 10-6	0.05 – 0.1 x 10-6
Carbonation Depth	mm	BS EN 14630, 2006 [14]	5 – 15	1 – 2	< 0.1
Abrasion Resistance	mm	ASTM C944-99, 2005 [15]	0.8 – 1.0	0.5 – 0.8	< 0.03
Water Absorption	%	BS1881-Part 122, 1983 [16]	> 3	1.5 – 3.0	< 0.2

Table 2 presents the mix design for the standard UHPdC with 2% steel fibers by volume of concrete. The high-range water reducing agent used is ***polycarboxylate ethers*** (PCE) based superplasticizer and no recycled wash water is used in the mixing. This mix design is set as a reference mix in this paper for comparison against other mix designs.

According to the concrete committee of Japan Society of Civil Engineering recommendation for design and construction of ultra-high strength fiber reinforced concrete structures [17], the steel fibers used are required to have a tensile strength of more than 2000 MPa. In addition, specimens or members made of ultra-high strength fiber reinforced concrete must be heat cured for 48 hours at a temperature of 90°C.

3.0 SUSTAINABILITY DESIGN APPROACH

3.1 Introduction

The approach used for the design of UHPdC structures is represented in Figure 2. The three criteria for assessment of a sustainable design are:

(i) Environmental impact calculation (EIC),
(ii) Durability design, and
(iii) Limit states design.

While there will be arguments as to the choice of an appropriate measure for sustainability, we shall adopt herein the environmental impact calculation (EIC). This criterion is a measure of the optimization of the materials used with respect to the embodied energy and CO_2 emission when compared to existing practice. In this paper is suggested that durability design be the sub-set of environmental impact design. Further, durability may be defined as the capability of a structure to meet its defined serviceability and strength limit state over time. Durability design is important to ensure the designed concrete structure meets the required design life, with as little maintenance as possible, thereby reducing the overall life-cycle cost, social impact and unplanned additional material consumption, which can bear heavily on future carbon impacts. Finally, the limit state design should be used to check for serviceability and strength requirements of the structure. If the aforementioned criteria can be adopted in any concrete structure design, the overall cost and functionality of a design structures can be optimized with minimum environmental impact.

3.2 Environmental Impact Calculation

Undertaking of a full environmental impact calculation (EIC) is a complex exercise and the data required for the calculation varies from country to country due to local practices and available technologies. Table 3 summarises the environmental data used in this comparative study. The table has been prepared for determining the equivalent CO_2 content of particular concrete mix designs and materials. The information may be updated frequently as the industry continues to improve its processes. The values of embodied energy (EE) and CO_2 emission in the production of the concrete and steel adopted for this study are extracted from the work of Struble and Godfrey [18] and are adapted as needed. According to Struble and Godfrey, the energy consumed in the production of Portland cement is estimated to be 4.88 MJ/kg and the total energy in the production of steel is estimated to be 23.7 MJ/kg (i.e. 185.8 GJ/m^3). Based on these values, the EE values of Grade-40 and Grade-60 concretes and of UHPdC with 1.5% and 2% of steel fibres can be determined and are presented in Table 3.

3.3 Example 1 – Single span 40m concrete road bridge

Figure 3 presents the layout of a single span 40m concrete bridge using both a conventional concrete design and an UHPdC design. The total transverse width of the bridge is 15m. Based on conventional concrete design, seven pieces of precast post-tensioned super-tee girders are needed. For the alternative UHPdC design, three U-girders are used (refer to Figure 4). In this example, the precast girders are designed to be simply supported at their ends and are composite with a 200 mm thick Grade-40 in-situ reinforced concrete (RC) deck slab. The RC deck is then covered with a 50 mm thick asphalt wearing surface. The bridge is designed for the following specifications:

- Design life: 120 years
- Exposure class: XS1- the superstructure of the bridge exposed to airborne salt but not in direct to contact with sea-water [19]
- Imposed live load: Load models 1 to 4 with special vehicle 1800/1500 [19]
- Minimum free-board clearance: 1.6m
- Superstructure: Precast girders with 200 mm thick composite in-situ RC deck slab
- Bridge length: Single span of 40 m
- Supported length: 39.5 m (centre-to-centre of bearings)
- Overall bridge width: 15 m
- Cross slope: 2.5 %

Figure 5 gives the detail of the alternative design U-precast girder. The 40m long girder consists of two 150 mm thick webs, a 200 mm thick base and it is post-tensioned using three tendons of 31S15 strands at the base and two tendons of 4S15 strands at the top flanges to ensure that the joints are in compression during transfer and in service. Each girder comprises five segments (three 8 m internal segments and two 8 m end-block segments). Unlike a conventional precast concrete girder, the webs do not contain any reinforcement for transverse shear forces with the steel fibres carrying the tensile component of the internal forces generated by shear [20, 21]. The girder weights 2.2 tonne/metre, which gives a total of 88 tonnes per girder.

Table 4 summaries the material quantities and EIC of the two bridge designs. In the calculation of the material quantity, only the superstructure is considered herein. The amount of EE and CO_2 emissions are obtained from multiplying the amount of materials by the environmental data given in Table 3. A comparison of the EIC results is presented in Figure 6. In terms of material consumption, the UHPdC solution consumed 37 % less material than the conventional solution. In terms of environmental impact, the UHPdC solution has 20% less embodied energy and 24% less CO_2 emissions. It also needs recognition that in this example only the savings at the level of the superstructure have been considered. Further savings will result from the lighter weight of the UHPdC solution giving a smaller substructure, foundations and lower transport costs.

3.4 Example 2 – UHPdC portal frame building

Figure 7 shows the construction of the world first portal frame building (Wilson Hall) using UHPdC technology [22]. The building was designed and built by Dura Technology Sdn. Bhd. in 2008, with the aim to study the potential use of UHPdC structural members against conventional steel members in portal frame construction. It is the company's goal to introduce this advanced, engineered and green material to Malaysia in a desire to bring the nation to a higher level in the innovation of building and construction technologies and to be considered as sustainable construction visionaries. In year 2010, the building has won a national record in the Malaysia Book of Record.

Wilson Hall consists of a total roof coverage area of 2,861 m^2. The total transverse width and longitudinal length of the building is 67 m and 42.7 m, respectively. Each portal frame is spaced 12.2 m centre-to-centre and the building consists of eight UHPdC prestressed columns, internal rafters, cantilever rafters and connectors as shown in Figure 8.

A comparison of the EIC results of the UHPdC portal frame against conventional steel portal frame solution is given in Table 5 and Figure 9. In terms of material consumption, the UHPdC portal frame system consumed 13% less material than the conventional steel portal frame solution. With regard to costs, the system is 16% more economical, whereas more cost savings can be realised in factory buildings that are located in corrosive environment or constantly subjected to chemical attack such as chemical plants and palm oil mills. In terms of environmental indexes, the UHPdC solution has 24 % less embodied energy and 19% less CO_2 emissions.

3.5 Example 3 – UHPdC short retaining wall

A total of 180 m long by 1.5 m high retaining wall was recently used in the construction of a 90 m long monsoon drain for a housing development project in Ipoh, Malaysia (Figure 10a). The vision of project owner saw clear advantages in providing an ultra-light weight and durable UHPdC retaining wall solution in lieu of an available conventional solution. The L-shaped wall comes with thin panels of 30 to 50 mm thick (Figure 10b). Unlike conventional RC L-shaped wall, which is precast in a standard 1 m length and weighs 1200 kg/m of wall. The UHPdC retaining wall is made in 3 m lengths (Figure 10c) and has a self-weight is just 260 kg/m, a factor of five times less than the conventional solution. Prior-to construction of the wall, the local council requested a load proof test on the wall with a surcharge load of 10 kPa at service and 15 kPa at ultimate. The wall was tested with back filled soil up to 1.5 m and an additional surcharge load of 25 kPa (Figure 10d), 66% greater than the strength limit requirement and still it did not fail! Thus, the wall performance was deemed to satisfy with the design service and strength requirements.

A comparison of the EIC results of the UHPdC retaining wall system against the conventional L-shaped RC wall is given in Figure 11. In terms of material consumption, the UHPdC retaining wall consumes 73% less material than the conventional RC wall. In terms of the environmental indexes, the UHPdC wall requires less embodied energy and produces 49% less CO_2 emissions. This it is another good example of how with innovative design UHPdC technology supports sustainable construction solutions.

4.0 DURABILITY DESIGN

Throughout the world there are many concrete structures suffering from corrosion, especially structures near coastal areas and in a marine environments. For example, some bridges have been demolished due to heavy corrosion at ages of just 20 to 30 years and, in some cases, the maintenance costs far outweighed the initial construction costs [23].

The most accepted model of service life concerning the corrosion of the reinforcing bars was developed by Tuutti [24]. Figure 12 shows the schematic evolution of damage of reinforced concrete structures due to steel corrosion. In this model, the service life is composed of two periods. First, the initiation period (t_i) relative to the penetration of the chlorides or carbon dioxide, i.e., the aggressive agents, until the depassivation and the beginning of the corrosion of the bars. Second is the propagation period (t_p) where corrosion occurs. Such a criterion proposes the service life to be determined as a function of an acceptable limit of corrosion.

$$Service\ Life = t_i + t_p \tag{1}$$

When modelling the initial phase, corrosion is triggered either by carbonation or when the critical corrosion-inducing chloride content is exceeded. The initial phase ends after the steel depassivation has started. Today, many well-tried models are available for the initial phase. Once steel depassivation has occurred, reinforcement corrosion must be taken into account in design with consideration of structural safety and is dependent on the material quality and the environmental conditions. The consequences of reinforcement corrosion in concrete are the loss of reinforcement cross-section, the development of tensile stress in concrete due to expansion caused by the by-products of the corrosion reaction and a change in the mechanical properties at the boundary between reinforcement and concrete. The effects of corrosion can be divided into those concerning the reinforcement, the surrounding concrete and the bond between the concrete and the steel.

Figure 12 shows a schematic on the evolution of damage due to reinforcement corrosion according to Tuutti [24]. It is not imperative that the limit states for cracking (Cr) and spalling (Sp) and loss of bonding (BL) are attained before the limiting loss of cross-section (CA) is reached. Rather, it is necessary to define the relevant limit state for the structural component within the grey area of the figure. For example, spalling of concrete can be an essential limit state for the design of a compressive strut member or in the region of anchorage of a steel bar whereas spalling of concrete cover in the middle region of beam under flexural load is less critical provided that the loss of steel cross-section of the longitudinal reinforcement is not significantly impacted.

On depassivation, two branches are possible. The first leads to loss of steel cross-section via pitting corrosion (acidification of the anode), the second to different states of damage via uniform surface corrosion. It should be noted that the surface corrosion of steel is always accompanied by a certain amount of pitting. Figure 12 shows that failure of bond divides into two different limit states. BL_1 describes the loss of bonding due to corrosion of the reinforcement ribs, leading to an undesirable slip of the reinforcement. The loss of bonding caused by spalling of concrete cover is defined by BL_2. According to Tuutti [24], both events are defined as limit states in Figure 12 and can as such be included in durability design.

A certain group of researchers propose the criterion that the service life be defined as the initiation of corrosion. The justification of this criterion is that once the corrosion has begun, the full process develops fast, especially in the case of attack by chlorides. The reason for such contention is that the second stage (i.e the propagation period) is an extremely complex subject due to a structure can has vast distinguished level of exposures, such as level of chlorides ingression, relative temperature and humidity, freeze and thaw attack, concrete grades, quality control during placing or manufacturing and many others to just list a few. Therefore in this paper, the service life of a structure is considered as the initiation period only as shown in Equation (2).

$$Service\ Life = t_i \tag{2}$$

Following is an example of the initial phase of steel depassivation due to chloride ion attack for NSC and HPC and for UHPdC. The concept of chloride attack due to chloride ions permeating into reinforced concrete are illustrated in Figure 14. The matrix of conventional concrete is analogous to that of a sponge (Figure 14) where the air voids, micro-pores, gel-pores and capillaries are inter-connected to each another. These micro-pores and gel water, which are generally formed in the concrete matrix, serve as routes for the movement of chloride ions. The pore structure in concrete depends on the type of concrete, mix proportion, type of formwork, placing technique, curing method, heat of hydration and material quality.

Near coastal areas, where high levels of air-borne chlorides exist, and where parts of structures lie in the splash zone, large quantities of chloride ions can adhere to the surface. The chloride ions then permeate and reach the concrete surrounding steel reinforcement. Chloride ions can break the passive oxide film and initiate corrosion even under highly alkaline condition. Thus, typical heavy cracking and spalling of concrete due to corrosion expansion of reinforcing steel may take place early (refer to Figure 15).

Unlike conventional concrete, UHPdC has a densely packed microstructure (Figure 14b) in which the water/binder ratio is lowered to below the hydration limit (W/B of 0.16 or less). Thus air voids are significantly reduced and are discontinuous in the matrix. Thechloride diffusion coefficient (D_c) of UHPdC is at least one order less than for conventional concrete. Therefore in the presence of chloride ions at the surface of the concrete, the amount of time needed for the chloride ions to diffuse through the concrete cover and initiate depassivation of the steel increases dramatically. Of course, this assumption is only valid provided the concrete is uncracked.

Taking the example as shown in Section 3.3, the durability aspect of the bridges using three different concrete grades is compared. According to [17] structures made of ultra-high strength fiber reinforced concrete shall have a minimum concrete cover of 20 mm and the concern on durability shall not be a major issue provided the concrete section is free from cracks. In contrast, according to EC2 clause 4.4 [25], the nominal concrete cover needed for the conventional HPC girder is 50 mm. The duration for a time needed for chloride ions diffuse through the concrete and start the corrosion process is not mentioned in design codes.

In this comparative study, the Grade 40 NSC, Grade 60 HPC and Grade150 UHPdC girders are assumed to have the same clear cover of 50 mm from the girder soffit, where both the bridges are exposed to airborne chloride ion attack. The durability is governed by Fick's 2nd law of diffusion [26], that is:

$$C_x = C_s \left[1 - erf\left(\frac{X}{2\sqrt{D_c\, t_i}}\right)\right] \tag{3}$$

where X is the distance of the outermost steel reinforcement from the concrete surface (in mm) also know as the concrete cover, t_i is the time (in seconds), D_c the diffusion coefficient (in mm^2/sec.), *erf* the error function, C_s the chloride ion concentration at the surface of the uncracked concrete and C_x is the critical chloride threshold concentration for steel corrosion.

The C_s value used in this example is the airborne chloride concentration based on the work by Yoshiki et al. [23]. The airborne chloride concentration $C_{s,airborne}$ (in kg/m^3) can be calculated from Equation (4) where D is the distance (in km) from the coast. Assuming the bridge is located 1m from the coast, then using Equation 4, the value of C_s = 6.4 kg/m^3.

$$C_{s,airborne} = \frac{1.22}{D^{0.24}} \quad where \quad 1m \le D \le 10km \tag{4}$$

Table 6 shows the critical chloride threshold concentration (C_x) value can range from 0.2% to 0.35% by weight of the cement content in the concrete mix. For comparison purpose, this paper adopted a value of 0.3% for the chloride threshold value.

Equation (3) is the simplest equation that expresses the process of chloride ingress from outside with the minimum required parameters. However, abundant data of C_s and D_c based on this model have been obtained from many kinds of tests and surveys to estimate existing structures. Otherwise, it is difficult to verify the validity of the model because time dependent nature of the data for various parameters such as temperature, humidity, carbonation, absorption into hydrated compounds and so on. Thus, Eq. (3) is appropriate for comparative purposes for the investigations of this paper.

The results in Table 7 show that with a concrete cover of 50 mm, and without intervention or any active corrosion prevention systems, corrosion initiation of the reinforcing steel in a Grade 40 NSC and Grade 60 HPC girder will occur after just after 2.1 and 7.5 year respectively. In contrast, a depassivation in an UHPdC girder will not start for 633 years. Even when the concrete cover of the HPC girder is increased to 100 mm, the time needed before the onset of corrosion increases to just 30 years. To meet the 120 year no maintenance criteria, a cover, in theory, of 200 mm would be required. Thus without regular maintenance, or passive or active corrosion protection systems, many concrete structures in marine environments fail at an early age. In comparison UHPdC structures have potential for significant savings in maintenance costs and a longer working life leading to sustainable solutions. This is particularly true if the structural element is pre-compressed to avoid cracking under service conditions.

5.0 CONCLUDING REMARKS

In this paper an overview is presented on the mechanical properties achieved for a Malaysia blend of UHPdC and examples of innovative construction solutions demonstrated. Three examples of environmental impact calculations for typical structures is provided for conventional and UHPdC solutions. The EIC results show that UHPdC structures are able to give immediate savings in terms of primary material consumption, embodied energy and CO_2 emissions. With regard to durability design, UHPdC structures are shown to be superior over conventional concrete. UHPdC structures have a much longer service life and design life without impact on the integrity or safety of a structure. The UHPdC technology is confirmed to be a greener construction material as it supports the vision of a sustainable construction future.

The authors are of the opinion that in the future, UHPdC technology will contribute significantly to the realisation of sustainable development. The technology carries an equation that sums up '*sustainable construction*' in that it provides for a minimum impact on the environment, maximizes structural performance and provides a minimum total life-cycle cost solution. The benefits are:

- Immediate reduction in overall consumption of non-renewable raw material (such as aggregate, sand and cement) thus directly result in lighter structures;
- Encourage the use of recycle materials (such as silica fume and GGBS);
- Better quality and finishes of finishing products;
- Prolong the service and design life of structures (and thus immediately eliminate the need of new replacement that required consumption of new materials, new budgeting cost and construction interruption to the public);
- Minimised maintenance due to the its superior durability (thus providing immediate savings in costs for repair and rehabilitation);
- Reduced overall CO_2 emissions, embodied energy and global warming potential through savings in material consumption;
- Old UHPdC structures that have reached the end of their service life can be recycled as good quality aggregate for production of new UHPdC members [30]; and
- The total life-cycle cost saving helps to relieve the future national economies.

Finally, UHPdC technology opens the door for new design approaches to conventional construction making concrete structure more sustainable, environmental friendly and providing lower life-cycle costs.

6.0 REFERENCES

[1] Richard, P. and Cheyrezy, M., 1995. Composition of reactive powder concretes. *Cement and Concrete Research*, 25 (7), 1501-1511.
[2] Richard, P. and Cheyrezy, M.H., 1994. Reactive powder concretes with high ductility and 200-800 MPa compressive strength. *ACI*, SP-144 (24), San Francisco, CA, 507-518.

[3] BS1881-Part 114, 1983. Testing concrete. Methods for determination of density of hardened concrete. British Standard, British Standards Institution, ISBN. 0-580-12948-9, 8.
[4] AS 1012.9, 1999. Determination of the compressive strength of concrete specimens. Australian Standard, Standards Australia, 12.
[5] BS6319-2, 1983. Testing of resin and polymer/cement compositions for use in construction. Method for measurement of compressive strength. British Standard, British Standards Institution, 4.
[6] AS1012.16, 1996. Determination of creep of concrete cylinders in compression. Australian Standard, Standards Australia, 8.
[7] BS1881-Part 121, 1983. Testing concrete. Methods for determination of static modulus of elasticity in compression. British Standard, British Standards Institution, 7.
[8] BS EN 12390-6, 2000. Testing hardened concrete. Tensile splitting strength of test specimens. British Standard, British Standards Institution, ISBN: 0-580-36606-5, 14.
[9] ASTM C496, 2004. Standard test method for splitting tensile strength of cylindrical concrete specimens. ASTM Standards, ASTM International, United States, 5.
[10] ASTM-C1018, 1997. Standard test method for flexural toughness and first crack strength of fiber reinforced concrete (using beam with third point loading). *ASTM Standards*, ASTM International, United States, 8.
[12] ASTM C1202, 2005. Standard test method for electrical indication of concrete's ability to resist chloride ion penetration. ASTM Standards, ASTM International, West Conshohocken, PA, 6.
[13] ASTM C1556, 2004. Standard test method for determining the apparent chloride diffusion coefficient of cementitious mixtures by bulk diffusion. ASTM Standards, ASTM International, United States, 7.
[14] BS EN 14630, 2006. Products and systems for the protection and repair of concrete structures. Test methods. Determination of carbonation depth in hardened concrete by the phenolphthalein method. British Standard, British Standards Institution, ISBN: 0-580-49622-8, 12.
[15] ASTM C944-99, 2005. Standard test method for abrasion resistance of concrete or mortar surfaces by the rotating-cutter method. ASTM Standards, ASTM International, United States, 4.
[16] BS1881-Part 122, 1983. Testing concrete. Method for determination of water absorption. British Standard, British Standards Institution, ISBN: 0-580-12959-4, 4.
[17] JSCE, 2006. Recommendations for design and construction of ultra high strength fiber reinforced concrete structures (draft). September, 2006, Concrete Committee of Japan Society of Civil Engineers (JSCE), JSCE Guideline for Concrete, No. 9, ISBN: 4-8106-0557-4, 106.
[18] Struble, J. and Godfrey, J. 2004. How sustainable is concrete? In: International Workshop on Sustainable Development and Concrete Technology, Beijing, May 20–21, 201-211.
[19] BS EN 1991-2, 2003. Eurocode 1: Actions on structures – Part 2: Traffic loads on bridges. British Standard, British Standards Institution, 162.
[20] Voo, Y.L, Foster, S.J., and Gilbert, R.I., 2006. Shear strength of fiber reinforced reactive powder concrete prestressed girders without stirrups. Journal of Advanced Concrete Technology, 4 (1), February, 123-132.
[21] Voo Y.L. and Foster S.J. 2009. Reactive powder concrete: analysis and design of RPC girders. Lambert Academic Publishing, 364, ISBN: 978-3-8383-2406-7.
[22] Voo, Y.L., and Poon, W.K., 2008. The world first portal frame building (Wilson Hall) constructed using ultra-high performance concrete" In: Proceedings of the 33rd Conference on Our World in Concrete & Structures (OWICS), 25th – 27th August, Singapore, 493-500.
[23] Yoshiki, T., et al., 2001. Study on required cover depth of concrete highway bridges in coastal environment. In: 17th US-Japan Bridge Engineering Workshops, 2001, Tsukuba, 1-16.
[24] Tuutti, K., 1982. Corrosion of steel in concrete. Swedish Cement and Concrete Research Institute, Nº F04, Stockholm, 469.
[25] BS EN 1992-2:2005. "Eurocode 2 – Design of concrete structures – Part 2: Concrete bridges – Design and detailing rules", British Standard, British Standards Institution, ISBN: 0 580 46576 4, 100 pp.
[26] Andrade, C., 1999. Chloride penetration model. In: International Specialist Workshop "Design of Durability of Concrete". Berlin, 15-16th June: Workshop Report, 13/10/1999, 103.
[27] BA 35/90: 1990 – The inspection and repair of concrete highway structures.
[28] BS8110: Part 1: 1997 – Structural use of concrete. Code of practice for design and construction
[29] Paul J. Tikalsky, David Pustka, and Pavel Marek, 2005, Statistical Variations in Chloride Diffusion in Concrete Bridges, ACI Structural Journal, May-June, pp 481 – 486.
[30] Sedran, T. Durand C., and Larrard, F. de, 2009. An example of UHPFRC recycling. In: Designing and *Building with UHPFRC: State of the Art and Development,* 17^{th}- 18^{th} November, Marseille, France, 1-9.

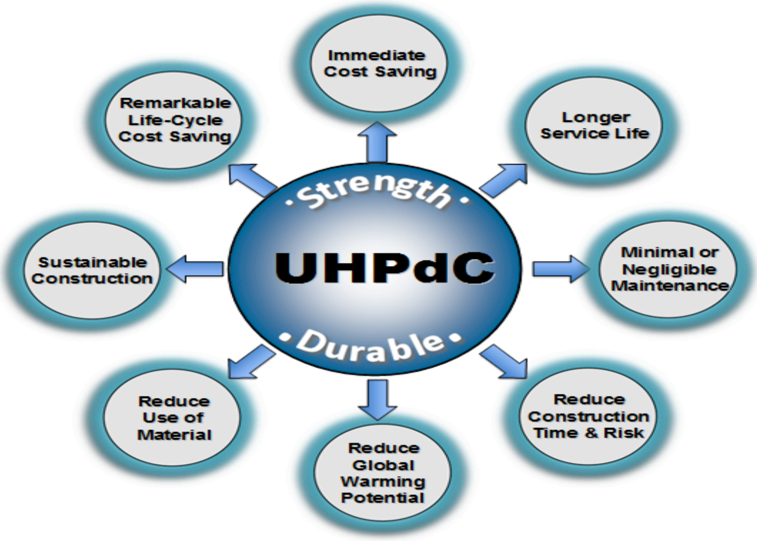

Figure 1 – UHPdC technology towards sustainable construction.

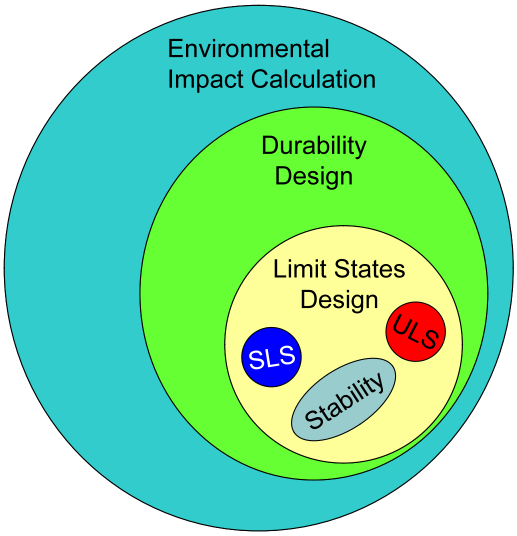

Figure 2 – Sustainable construction design models

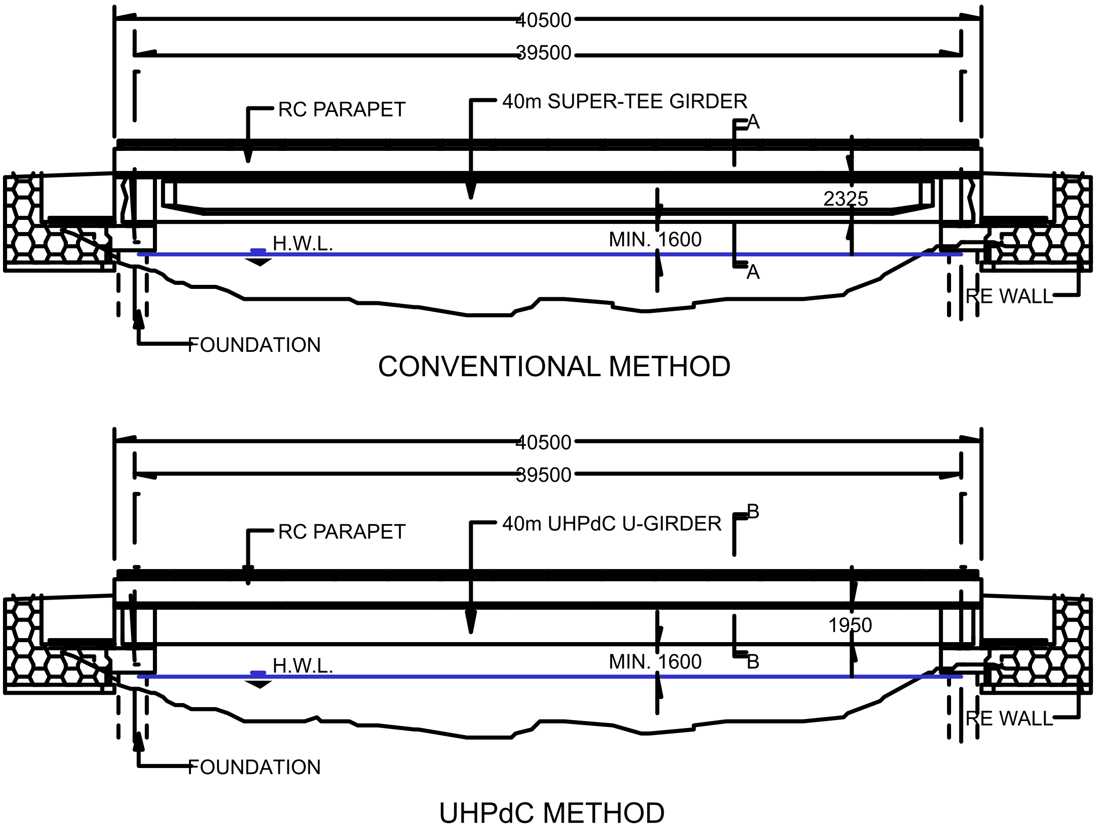

Figure 3 – Layout of a 40m span concrete road bridge

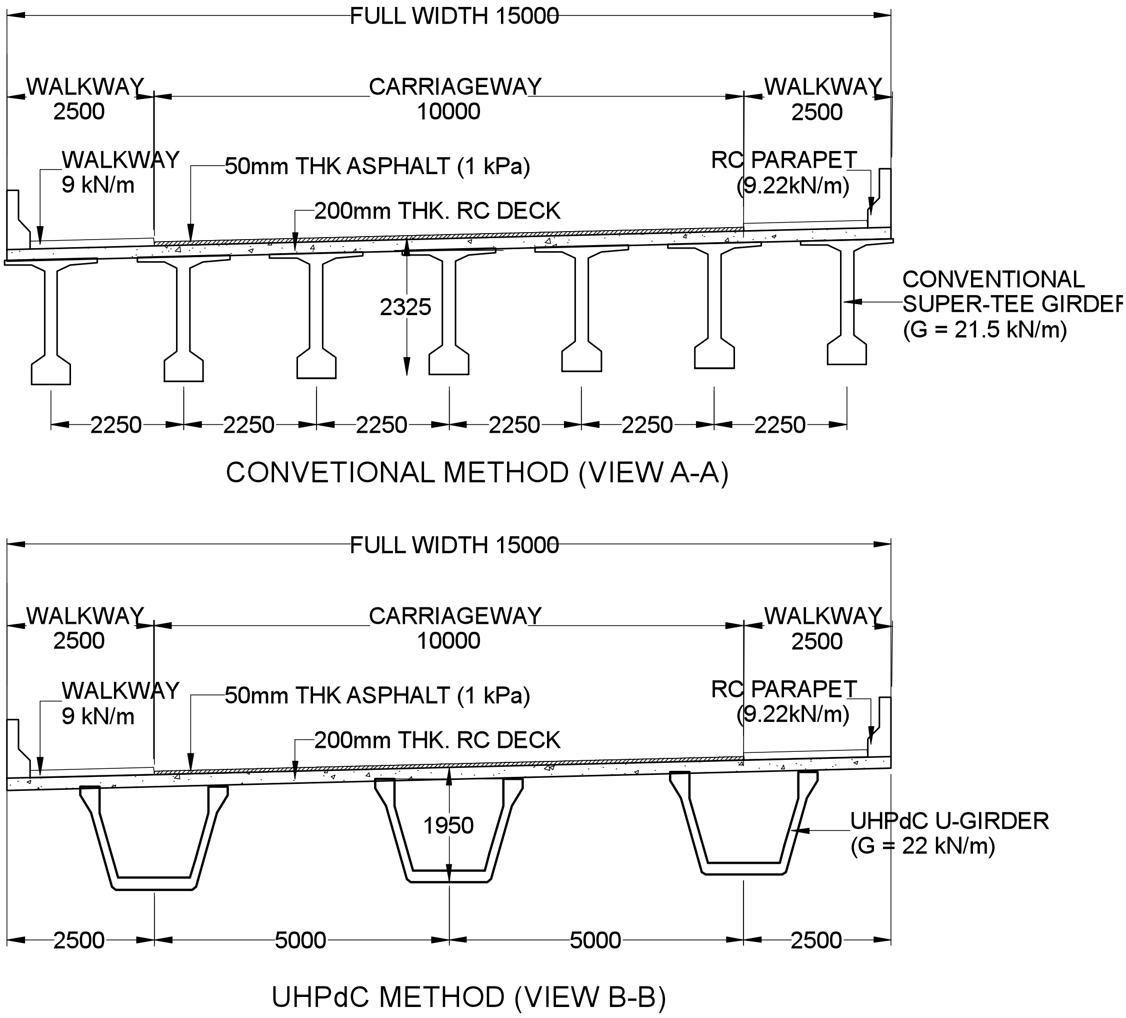

Figure 4 – Cross-sectional view

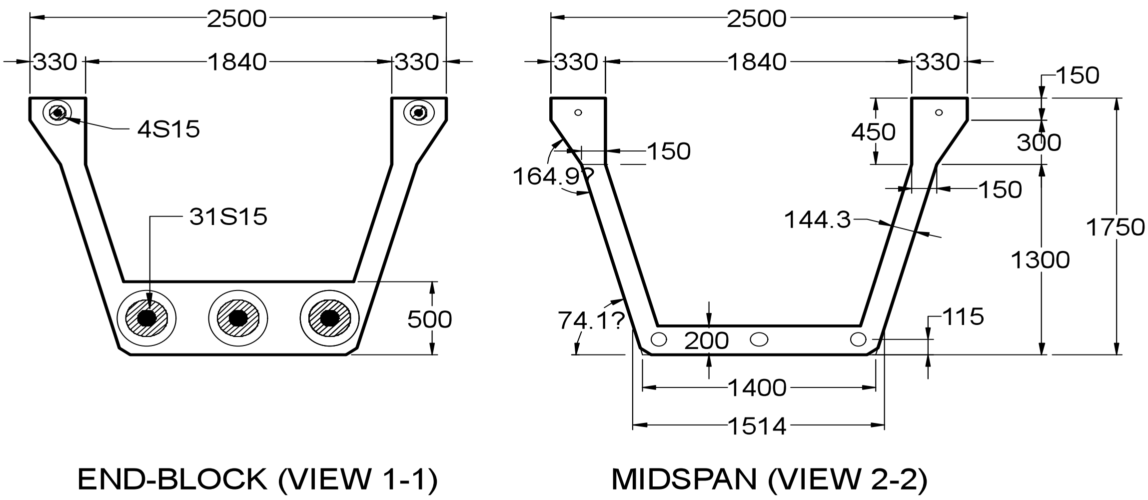

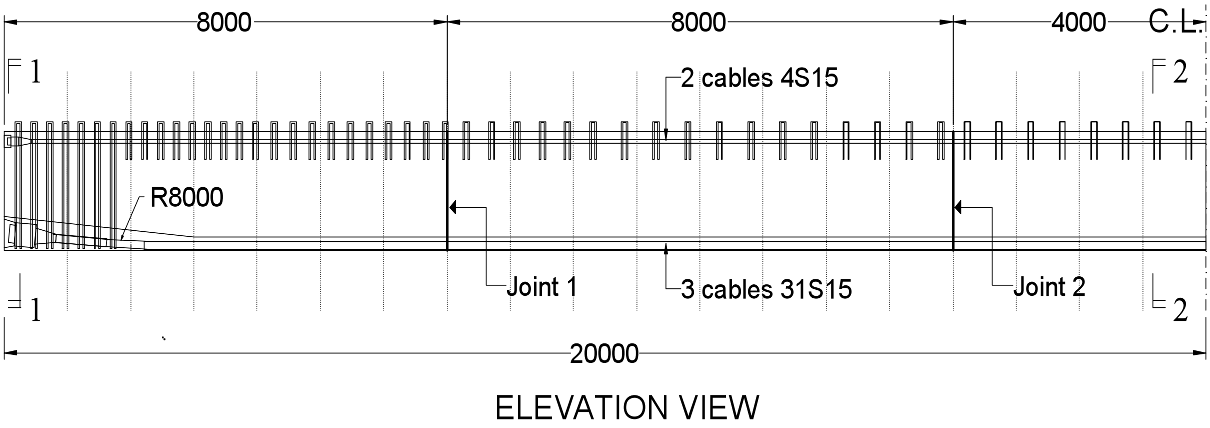

Figure 5 – Dimension of DURA®- U1750-40 bridge girder.

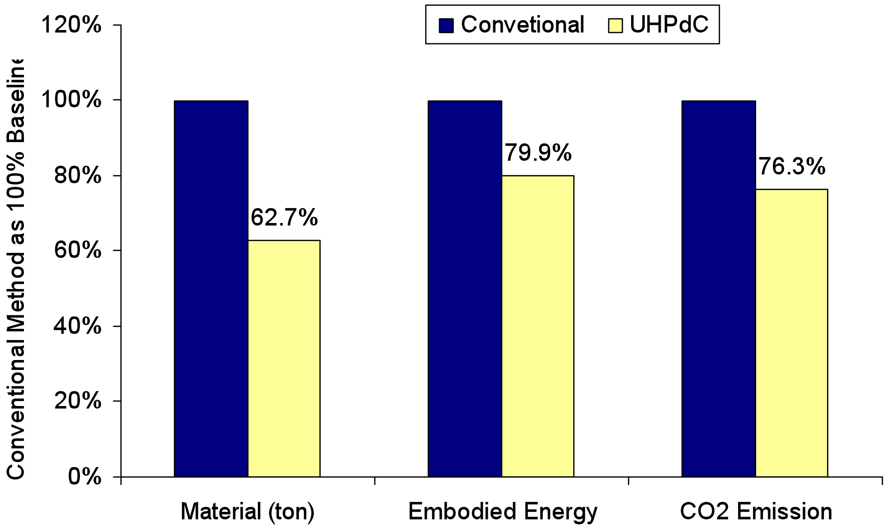

Figure 6 – EIC comparison for 40 m span bridges

Figure 7 - DURA®-UHPdC portal frame.

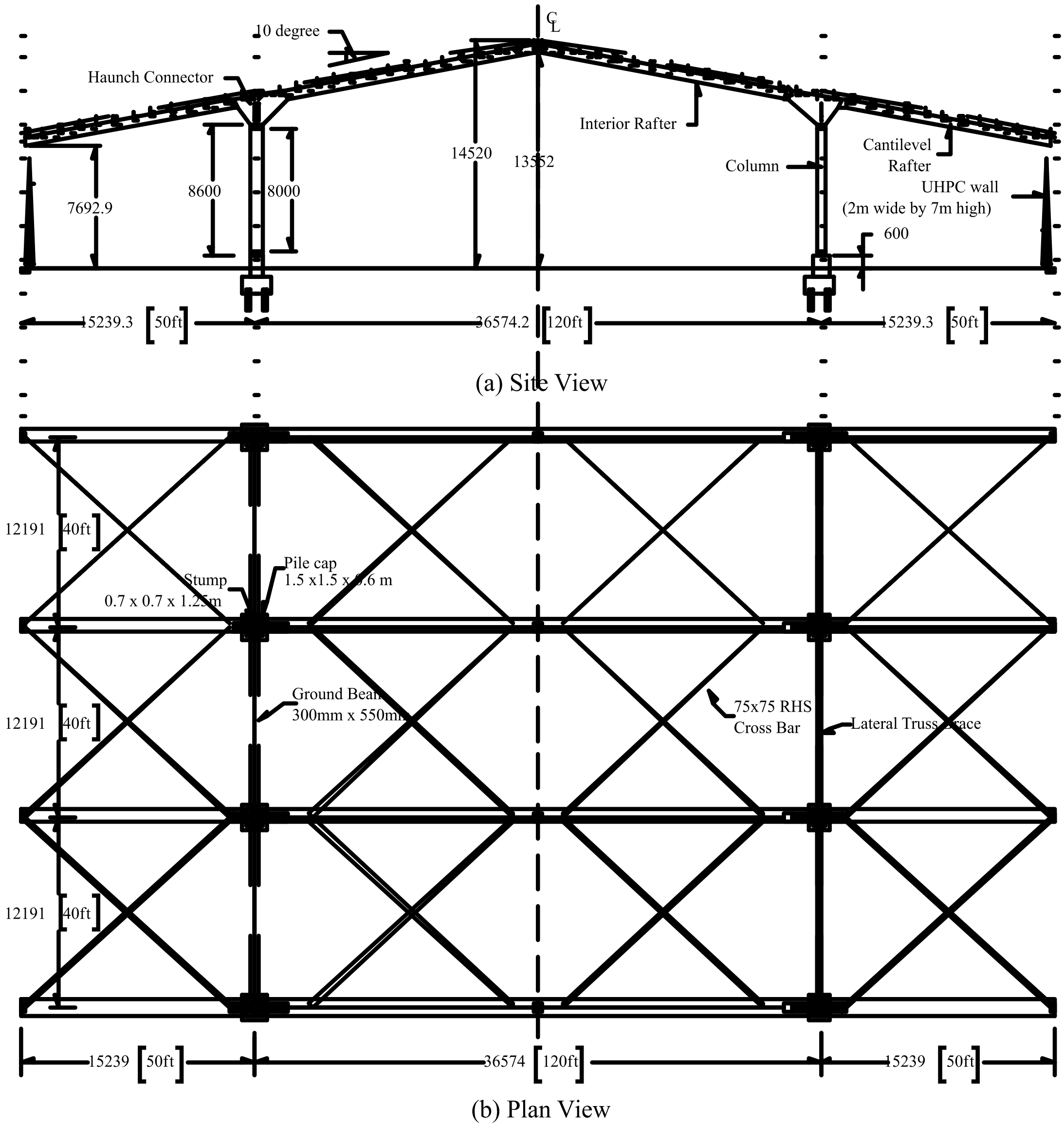

Figure 8 – a) Side view and (b) plan view of Wilson Hall.

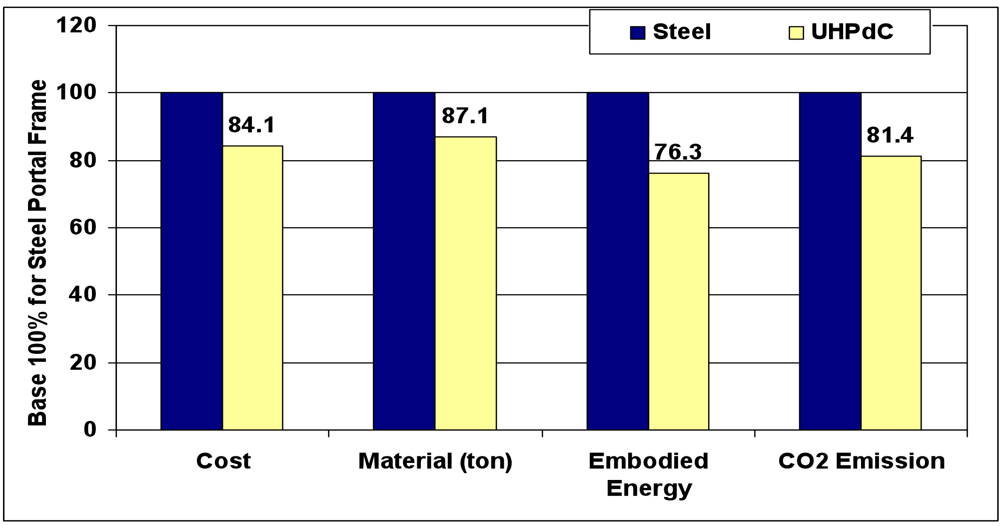

Figure 9 – EIC of portal frame buildings.

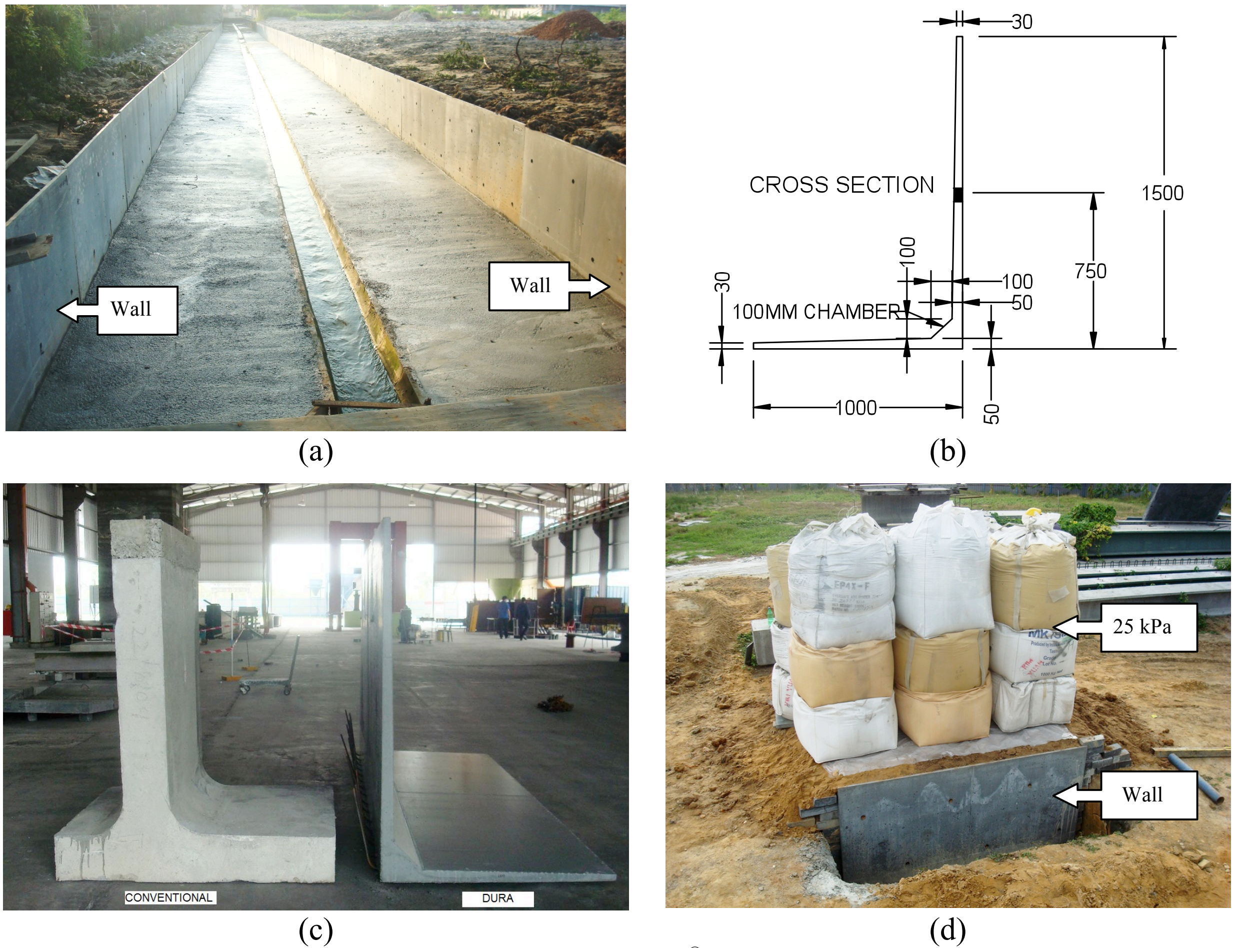

Figure 10 – (a) 90 m long monsoon drain using DURA® retaining wall, (b) cross-section detail; (c) comparison of conventional precast L-shape retaining wall against ultra-light weight DURA® retaining wall, and (d) load proof test of the wall back filled and with a 25 kPa surcharge load.

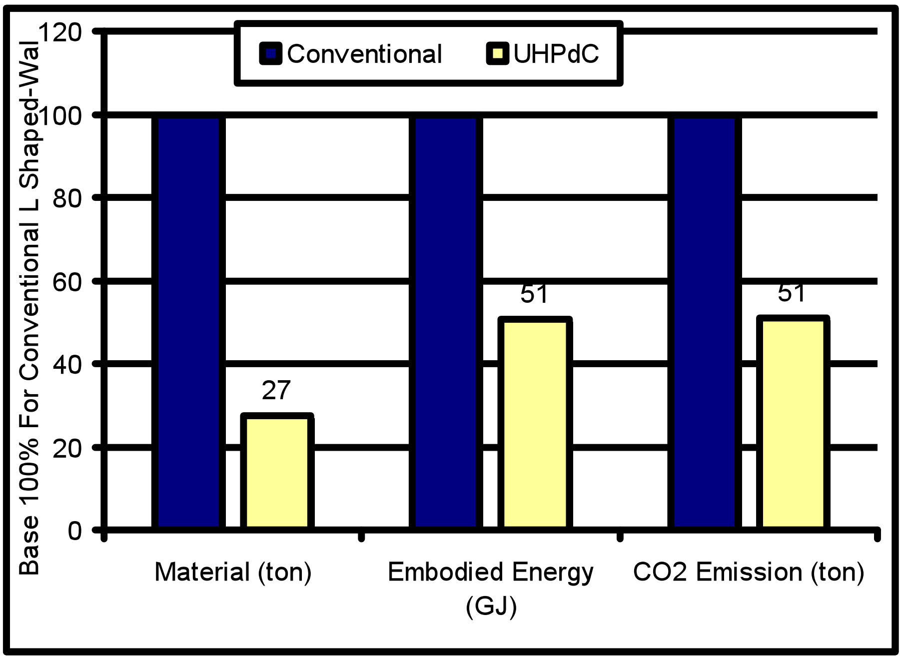

Figure 11 – EIC of retaining walls.

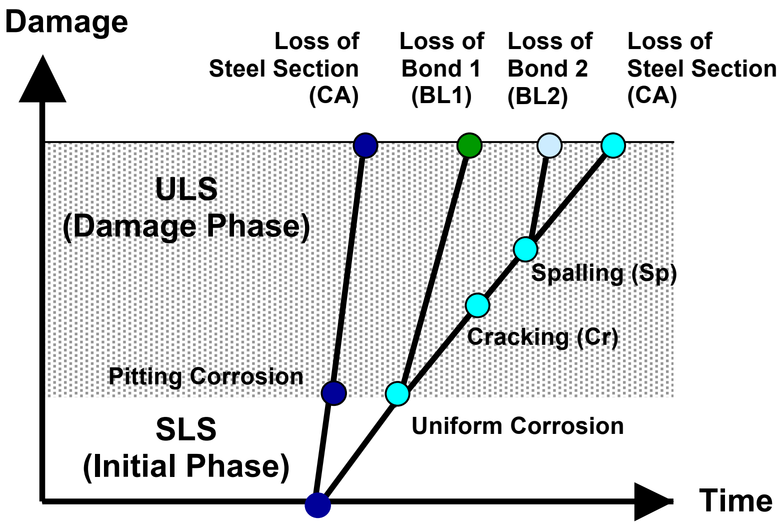

Figure 12 – Schematic representation of the evolution of damage of reinforced concrete structures due to corrosion [24].

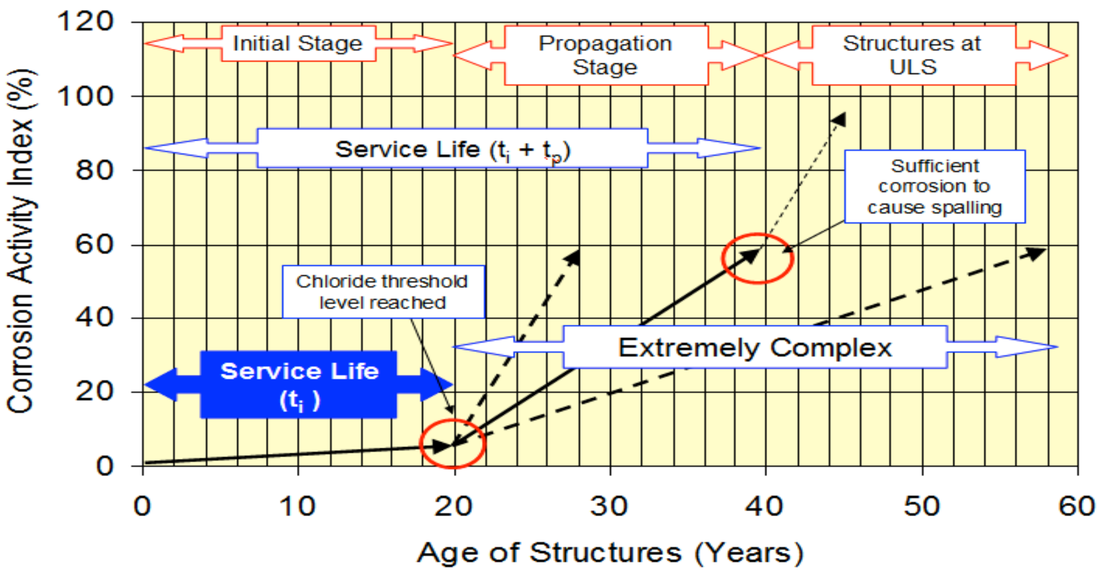

Figure 13 – Corrosion model of RC structures

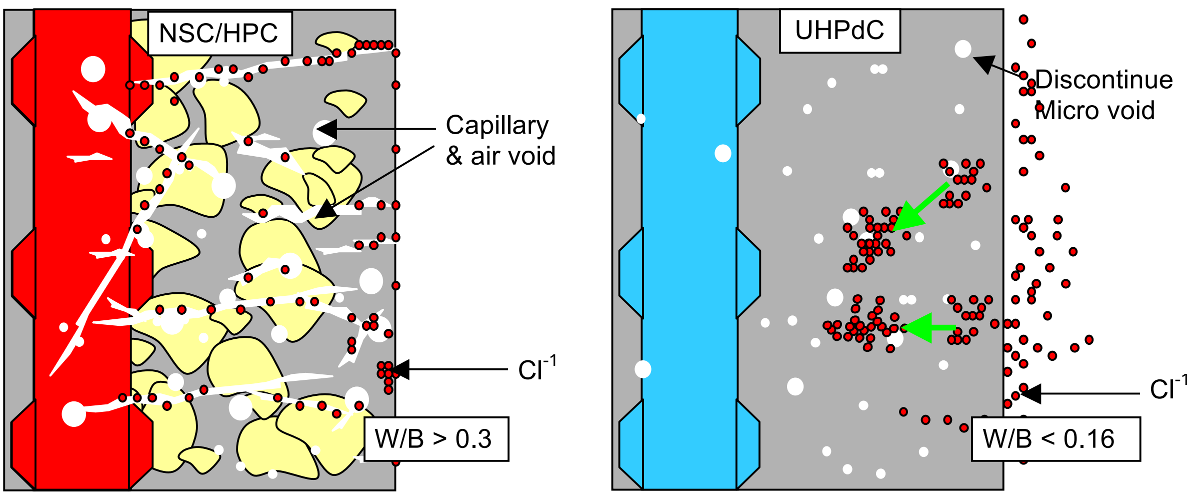

(a) (b)

Figure 14 – Comparison of concrete matrix of (a) ordinary concrete against (b) UHPdC.

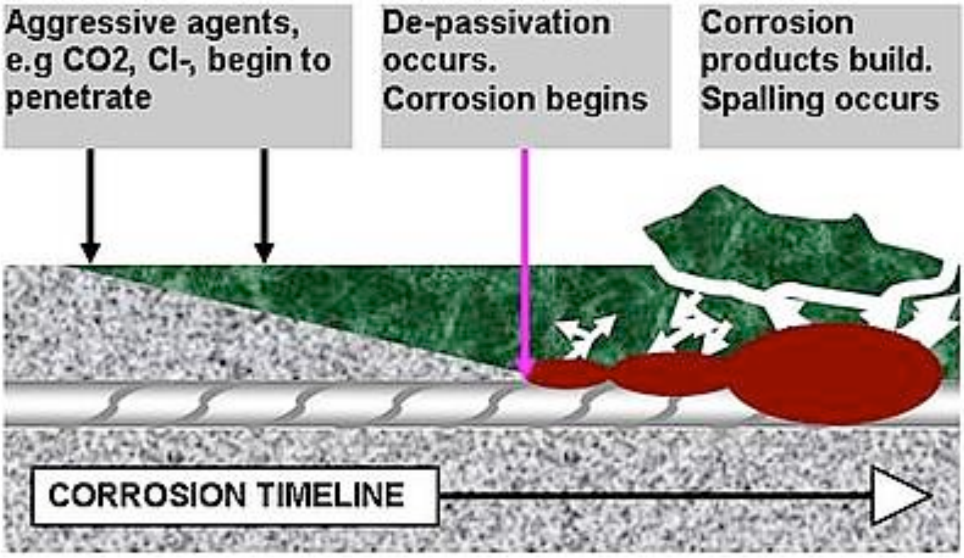

Figure 15 – Schematic showing timeline of concrete spalling due to steel corrosion.

Table 1 – Material characteristics of UHPdC compared to normal strength concrete (NSC) and high performance concrete (HPC)

Characteristics	Unit	Codes / Standards	NSC	HPC	DURA® - UHPdC
Specific Density, □	kg/m³	BS1881-Part 114, 1983 [3]	2300	2400	2350 – 2450
Cylinder Compressive Strength, f_{cy}	MPa	AS1012.9, 1999 [4]	20 – 50	50 – 100	120 – 160
Cube Compressive Strength, f_{cc}	MPa	BS6319-Part 2, 1983 [5]	20 – 50	50 – 100	130 – 170
Creep Coefficient at 28 days, □$_{cc}$		AS1012.16, 1996 [6]	2 – 5	1 – 2	0.2 – 0.5
Post Cured Shrinkage	□□	AS1012.16, 1996 [6]	1000 – 2000	500 – 1000	< 100
Modulus of Elasticity, E_o	GPa	BS1881-Part 121, 1983 [7]	20 – 35	35 – 40	40 – 50
Poisson's Ratio, □			0.2	0.2	0.18 – 0.2
Split Cyl. Cracking Strength, f_t	MPa	BS EN 12390-6, 2000 [8] ASTM C496, 2004 [9]	2 – 4	4 – 6	5 – 10
Split Cyl. Ultimate Strength, f_{sp}	MPa		2 – 4	4 – 6	10 – 18
Flexural 1st Cracking Strength, $f_{cr,4P}$	MPa	ASTM C1018, 1997 [10] (Four-Point Test on Un-notched Specimen)	2.5 – 4	4 – 8	8 – 9.3
Modulus of Rupture, $f_{cf,4P}$	MPa		2.5 – 4	4 – 8	18 – 35
Bending Fracture Energy, $G_{f,□=0.46mm}$	N/mm		< 0.1	< 0.2	1 – 2.5
Bending Fracture Energy, $G_{f,□=3.0mm}$	N/mm		< 0.1	< 0.2	10 – 20
Bending Fracture Energy, $G_{f,□=10mm}$	N/mm		< 0.1	< 0.2	15 – 30
Toughness I_5			1	1	4 – 6
Toughness I_{10}			1	1	10 – 15

Indexes I_{20}			1	1	20 – 35
Modulus of Rupture, $f_{cf,3P}$	MPa	JCI-S-002, 2003 [11] (Three-Point Test on Notched Specimen)	2.5 – 4	4 – 8	18 – 35
Bending Fracture Energy, $G_{f,\square=0.46mm}$	N/mm		<0.1	<0.2	1 – 2.5
Bending Fracture Energy, $G_{f,\square=3.0mm}$	N/mm		<0.1	<0.2	10 – 20
Bending Fracture Energy, $G_{f,\square=10mm}$	N/mm		<0.1	<0.2	15 – 30
Rapid Chloride Permeability	coulomb	ASTM C1202, 2005 [12]	2000 – 4000	500 – 1000	< 200
Chloride Diffusion Coefficient, D_c	mm^2/s	ASTM C1556, 2004 [13]	$4 – 8 \times 10^{-6}$	$1 – 4 \times 10^{-6}$	$0.05 – 0.1 \times 10^{-6}$
Carbonation Depth	mm	BS EN 14630, 2006 [14]	5 – 15	1 – 2	< 0.1
Abrasion Resistance	mm	ASTM C944-99, 2005 [15]	0.8 – 1.0	0.5 – 0.8	< 0.03
Water Absorption	%	BS1881-Part 122, 1983 [16]	> 3	1.5 – 3.0	< 0.2

Table 2 - Mix design of standard DURA®-UHPdC (quantity in kg/m^3)

Ingredient	**Mass (kg/m^3)**
DURA®-UHPdC Premix	2100
Superplasticizer	40
High strength steel fibers	157
Free water	144
3% moisture	30
Targeted W/B ratio	0.15
Total air voids	< 4%

Table 3 – Environmental data for environmental impact calculation (EIC)

	Cement Content	**Density**	**EE**	**CO_2**	**EE**	**CO_2**
Units	kg/m^3	kg/m^3	GJ/m^3	kg/m^3	MJ/kg	kg/kg
UHPdC (c/w 1.5% Steel Fiber)□	720	2350	6.814	982	2.90	0.418
UHPdC (c/w 2% Steel Fiber)□	720	2400	7.77	1065	3.24	0.44
Grade-60 (15% PFA)	480	2350	2.70	480	1.15	0.20
Grade-40 (15% PFA)	350	2350	1.73	297.5	0.74	0.13
P.C. Strands	-	7840	185.8	17123	23.7	2.18
Reinforcement	-	7840	185.8	17123	23.7	2.18

□Environmental values include steel fiber contribution

Table 4 – Material quantities and environmental impact calculation for Example 1.

		UHPdC (m^3)	Grade 60 Concrete (m^3)	Grade 40 Concrete (m^3)	Strands (tonne)	Reo. (tonne)	
No.	**Conventional Concrete Design**						
1	Precast 40m T- girders	0	308	0	16.03	31.92	
2	End crosshead (inc. wingwall, approach slab and diaphragm)	0	0	124.9	0	16.61	
3	R.C. deck (total)-1.5% Reo.	0	0	120	0	14.1	
4	R.C. Parapet-1.0% Reo.	0	0	31.3	0	2.45	
	Sub-Total	0	308	276	16	65	**Total**
A	**Mass of material used (tonne)**	0	724	649	16.0	65.1	**1454**
B	**Embodied energy (GJ)**	0	832	479	380	1543	**3233**
C	**CO_2 (tonne)**	0	148	82	35	142	**407**
No.	**UHPdC Design**						
1	Precast 40m U-girders	108	0	0	13.5	3.6	
2	End crosshead (including wingwall, approach slab and diaphragm)	0	0	103	0	16.61	
3	R.C. deck (total) - 2% Reo.	0	0	120	0	18.8	
4	R.C. Parapet-1.0% Reo.	0	0	31.3	0	2.45	
	Sub-Total	108.0	0.0	254.2	13.5	41.5	**Total**
A	**Mass of material used (tonne)**	259	0	597	13.5	41.5	**911**
B	**Embodied energy (GJ)**	839	0	441	320	983	**2583**
C	**CO_2 (tonne)**	115	0	76	29	91	**311**

Table 5 – Material quantities and EIC for Example 2 on portal frames

	Conventional	**UHPdC**
Raw Material (tonne)	1403	1222
Steel (tonne)	116	80
Cement (tonne)	158	192
Embodied Energy (GJ)	3707	2830
CO_2 Emission (tonne)	417	340
100-years GWP (tonne)	946	793
Cost of building (Ringgit Malaysia)	722,728 (year 2007)	608,052 (year 2008)

Total mass of material consumption for the portal frame, metal roofing, purlins, lateral and cross bracing, bolting, stiffeners, wall cladding, reinforced concrete slab and beams and pile caps (but excluded piling).

Table 6 – Chloride threshold corresponding to concrete grade

		C_x		
Code	C_x (% by wt. of cement)	G40 (kg/m^3)	G60 (kg/m^3)	G150 (kg/m^3)
Cement Content	-	350	480	720
BA 35/90 (1990) [27]	**0.30**	**1.05**	**1.44**	**2.16**
BS8110: Part1 [28]	0.35	1.23	1.68	2.52
Paul et al. (2005) [29]	0.20	0.7	0.96	1.44

Table 7 – Durability calculation in marine environment (for air-borne salt)

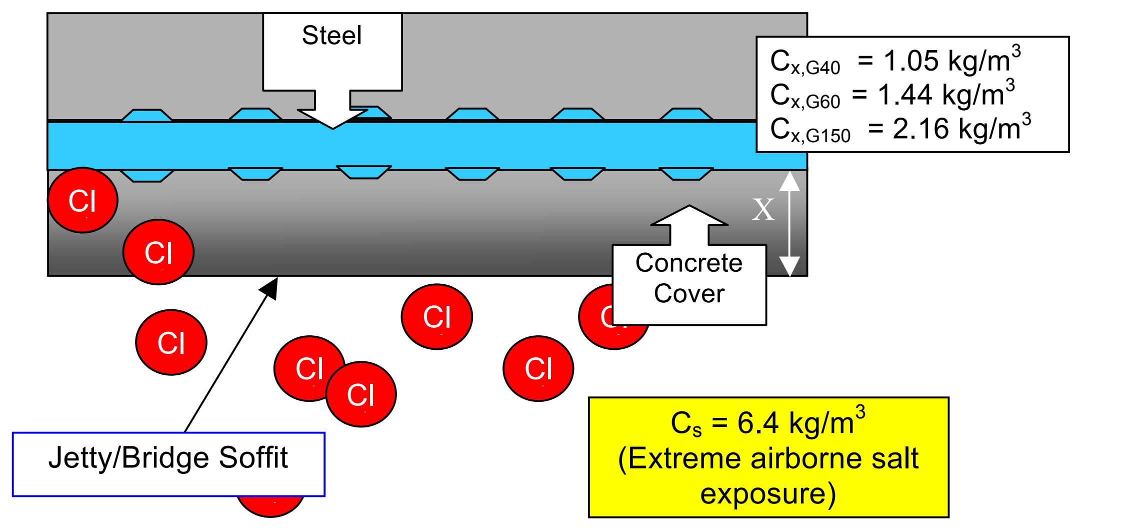

	NSC	**HPC**	**UHPdC**
Concrete characteristic strength (MPa), f_{ck}	40	60	150
Concrete cover, X (mm)	50	50	50
Airborne chloride concentration, C_s (kg/m^3)	6.4	6.4	6.4
Chloride threshold concentration, C_x (kg/m^3) (refer to Table 6)	1.05	1.44	2.16
Chloride diffusion coefficient, D_c (mm^2/s)	8×10^{-6}	3×10^{-6}	6.78×10^{-8}
Time (years), t_i	2.55	8.95	633
Time / 120 years design life (%)	2.1	7.5	528